J Mater Sci (2007) 42:5182–5187
DOI 10.1007/s10853-006-0542-5

A comparison of impression and compression creep behavior of polycrystalline Sn

C. Park · X. Long · S. Haberman · S. Ma · I. Dutta · R. Mahajan · S. G. Jadhav

Received: 23 February 2006 / Accepted: 7 June 2006 / Published online: 23 February 2007

Abstract This paper reports on the application of a miniaturized impression creep test to measure the creep behavior of pure polycrystalline Sn, and compares the results to compression creep data on the same sample, in order to experimentally determine a scaling constant to formulate the equivalent uniaxial creep constitutive law from the impression creep data. The creep parameters determined via impression and compression creep are found to be identical, with n ~ 5 and Q ~ 42 kJ/mol, indicating that over the tested stress–temperature range, the mechanism is core diffusion controlled dislocation creep. In conjunction with results from previous modeling work, a single conversion factor, κ^n/C, which depends on material properties, is shown to be usable for converting the impression creep relation to the equivalent uniaxial creep relation, and the experimentally determined value of κ^n/C for polycrystalline Sn is very close to that obtained via modeling.

Introduction

Sn-rich alloys (e.g., Sn–3.5 wt.% Ag and Sn–4 wt.% Ag–0.5 wt.% Cu) constitute popular lead-free solder materials for microelectronic packaging due to their easy processability, good mechanical properties and relatively low cost. The creep properties of Sn or Sn-based alloys are critical to the reliability of modern microelectronic solders, which are subjected to high homologous temperatures and large thermo-mechanical stresses during service [1]. The creep behavior of pure Sn, in both single-crystal and polycrystalline form, has been widely studied [2–7]. Recently, there has been a resurgence of interest in the mechanical properties of Sn, since the creep response of the new-generation of Sn-rich solders based on Sn–Ag or Sn–Ag–Cu eutectics is mechanistically similar to that of pure Sn [8]. There has also been significant interest in developing a miniaturized impression creep test to directly characterize individual microscale solder balls attached to a microelectronic packaging substrate [9–12], since it has been observed that the microstructures, and hence the creep behavior of bulk samples used in conventional creep tests are quite different from those of tiny microelectronic solder joints. In this paper, we report on the application of the miniaturized impression creep test to measure the creep behavior of pure polycrystalline Sn, and compare the results to compression creep data on the same sample, in order to experimentally determine a scaling constant to formulate the equivalent uniaxial creep constitutive law from the impression creep data.

C. Park · X. Long · S. Haberman · S. Ma ·
I. Dutta (✉)
Department of Mechanical & Astronautical Engineering,
Center for Materials Science and Engineering,
Naval Postgraduate School, Monterey, CA 93940, USA
e-mail: idutta@nps.edu

R. Mahajan · S. G. Jadhav
Intel Corporation, Assembly Technology Development,
5000 West Chandler Boulevard, Chandler, AZ 85226, USA

Background

The impression creep test, wherein a cylindrical punch is utilized to load the solder balls under nominal compression [13, 14], allows steady state creep to be established quickly, while enabling multiple creep curves to be generated from the same sample, thus proffering increased testing throughput relative to conventional uniaxial creep tests. The correspondence between impression creep results and uniaxial creep data, is therefore of substantial interest.

For a material undergoing power-law creep, the creep rate is given by:

$$\dot{\varepsilon} = A_1 \left(\frac{Gb}{kT}\right) \left(\frac{\sigma}{G}\right)^n e^{-Q/RT} \tag{1}$$

where A_1 is the Dorn constant, σ is applied stress, k is Boltzmann's constant, b is Burgers vector, Q is the activation energy, R is the gas constant, T is the absolute temperature, and G is the shear modulus. Correspondingly, an impression creep test yields the impression velocity (V) versus punch stress (σ_p) data, given by:

$$V = A_2 \left(\frac{Gb}{kT}\right) \left(\frac{\sigma_P}{G}\right)^n e^{-Q/RT} \tag{2}$$

where $A_2 = A_1 \cdot f(\varphi)$, and $f(\varphi)$, the effective gauge length for the impression creep test, is a function of the indenter diameter φ. Thus, the impression creep test directly yields the creep stress exponent n and the activation energy Q. Further, it is generally accepted that the function f depends linearly on φ, and equals $C\varphi$, C being a constant with a typical value in the range of 0.5–1.5 [15–21]. The equivalent uniaxial creep strain rate during impression creep may therefore be expressed as:

$$\dot{\varepsilon} = V/C\phi \tag{3}$$

Likewise, the punch stress σ_p is proportional to the equivalent uniaxial stress σ, yielding:

$$\sigma_p = \kappa\sigma \tag{4}$$

where the constant κ has typical values of in the range of 2–4 [15–21].

Substituting Eq. 4 into 2 and combining with Eq. 3, one obtains:

$$\dot{\varepsilon} = \frac{V}{C\phi} = \frac{A_2}{C\phi} \left(\frac{Gb}{kT}\right) \left(\frac{\kappa\sigma}{G}\right)^n e^{-Q/RT} = \frac{A_2\kappa^n}{\phi C} \left(\frac{Gb}{kT}\right) \left(\frac{\sigma}{G}\right)^n e^{-Q/RT} \tag{5}$$

Comparing Eq. 5 with Eq. 1, it is observed that the Dorn constant A_1 in the creep equation (Eq. 1) may be expressed in terms of the pre-exponent A_2 in the impression creep equation as:

$$A_1 = \frac{A_2\kappa^n}{\phi C} \tag{6}$$

Thus, if κ and C are known individually, or the term κ^n/C is known for a given material, the impression creep results (based on a known punch diameter φ) can be directly converted into the equivalent uniaxial data.

However, because of complications due to material property dependence of κ and C, only limited attempts have been made to determine their values [15–21]. In general, this has been accomplished either by (i) comparing the monotonic σ–ε behavior obtained via uniaxial testing with the σ_p versus nominal impression strain (given by $\delta/C\varphi$, where δ is the impression depth and $C \approx 1$) response during monotonic impression loading under plasticity conditions [17–19], or by (ii) finite element (FE) model based comparison of the impression creep velocity function with the constitutive creep law [22–23]. Since the material under the punch can creep even in the absence of plastic deformation (and hence the geometry of the crept zone can be quite different from that of the plastically deformed zone), the conversion factors obtained from monotonic tests are unlikely to be strictly applicable to creep. On the other hand, FE-model based conversions, which are typically valid for narrow conditions and limited material properties, are not available for Sn, nor have the approaches themselves been validated experimentally. Therefore, in this work, we seek (a) to experimentally characterize the creep behavior of polycrystalline Sn by both impression and compression creep tests, and (b) to establish a single conversion factor (κ^n/C) for polycrystalline Sn which will enable conversion of impression creep behavior to the equivalent uniaxial creep law.

Experimental

Virgin Sn (99.999% pure) was melted at 673 K, and poured into two 3 mm diameter, 8 mm deep holes in a graphite mold pre-heated to 533 K. Immediately after pouring, the mold was quenched in a mixture of methanol and liquid nitrogen at 223 K, producing an approximate cooling rate of 20 K/s. The samples were then cut into 3 mm lengths to produce cylinders of aspect ratio 1, and the ends were ground to a 6 μm finish. The same sample geometry was used for both impression and compression creep tests.

Impression creep tests were conducted using a 100 μm diameter tungsten carbide punch in conjunction with a miniaturized impression creep test set-up developed for testing solder balls attached to printed circuit boards. Details of the impression test apparatus and procedure are available elsewhere [1, 9–12]. Compression creep tests were conducted under constant load condition using a servo-hydraulic test frame equipped with a capacitance displacement gauge. In order to minimize sticking friction, thin graphite sheets were used to lubricate the sample ends while testing. The test temperature ranged from 323 to 423 K for both impression and compression tests, the σ_p range for impression tests was 10–50 MPa, and the nominal σ range for compression tests was 3–20 MPa.[1] Since the sample diameter increased during compression tests, the true creep stress decreased during the test. For analysis, the true stress was taken to be the mean value of the stress during apparent steady-state creep, where the stress change was quite slow.

Results and discussion

Figure 1 shows the microstructure of polycrystalline Sn used in the present study. The average grain size in the sample is observed to be about 20–30 μm. Since the crept zone during impression creep is roughly spherical with a diameter of ~2φ (i.e., ~200 μm for the present experiments) (Long X, Pan D, Dutta I, unpublished research, manuscript in review), the impression creep results are based on a volume comprising ~100 grains, thereby ensuring that the measured properties are representative of polycrystalline Sn.

Since A_2, b and k are constant, Eq. 2 allows us to obtain the stress exponent n from a plot of ln(VT/G) versus σ_p/G at constant T, and the activation energy Q from a plot of ln(VT/G) versus 1/RT at constant σ_p/G, where G represents the temperature-dependent shear modulus of Sn, given by G (MPa) = 20,632 – 37.67T (°C) [24]. These plots are shown in Fig. 2a and b, which show that n = 4.8 ± 0.08, and Q = 42.7 ± 3.65 kJ/mol. Re-writing Eq. 2 we have:

$$\frac{VT}{G\phi} = \frac{A_2}{\phi}\left(\frac{b}{k}\right)\left(\frac{\sigma_P}{G}\right)^n e^{-Q/RT}, \text{ or } \frac{VT}{G\phi}e^{Q/RT} = \frac{A_2}{\phi}\left(\frac{b}{k}\right)\left(\frac{\sigma_P}{G}\right)^n = A_{imp}\left(\frac{\sigma_P}{G}\right)^n \quad (7)$$

The pre-exponential constant A_{imp}, which equals $\frac{A_2}{\phi}\left(\frac{b}{k}\right)$, may then be determined from a plot of the temperature-compensated nominal strain rate during impression creep, (VT/Gφ)exp(Q/RT), versus the modulus-compensated punch stress σ_p/G with constant Q, as shown in Fig. 2c for Q = 42 kJ/mol. Regression analysis of all the data in Fig. 2c gives n = 5.076 and A_{imp} = 1.7 × 10^{12} K/(MPa-s).[2]

For compression creep, we may re-write Eq. 1 as:

$$\frac{\dot{\varepsilon}T}{G} = A_1\left(\frac{b}{k}\right)\left(\frac{\sigma}{G}\right)^n e^{-Q/RT}, \text{ or } \frac{\dot{\varepsilon}T}{G}e^{Q/RT} = A_1\left(\frac{b}{k}\right)\left(\frac{\sigma}{G}\right)^n = A\left(\frac{\sigma}{G}\right)^n \quad (8)$$

Similarly to the treatment of impression creep data, n and Q values for compression creep may be obtained by plotting ln($\dot{\varepsilon}$T/G) versus σ/G, and ln($\dot{\varepsilon}$T/G) versus 1/RT. This is shown in Fig. 3a and b, which give n = 4.92 ± 0.03, and Q = 41 kJ/mol.[3] As shown in Eq. 8, the pre-exponential constant A, which equals $A_1\left(\frac{b}{k}\right)$, may now be obtained by plotting the temperature-compensated strain rate ($\dot{\varepsilon}T/G$) exp(Q/RT)) versus the modulus-compensated stress σ/G, as shown in Fig. 3c, assuming Q = 42 kJ/mol (i.e., the same as that for impression creep). It is observed that the fit is very good, and yields n and A values of 5.05 (R = 0.892) and 1.6 × 10^{15} ± 1.58 × 10^{14} K/(MPa-s), respectively, for compression creep.[4]

Figure 4 shows plots of ($\dot{\varepsilon}T/G$) exp(Q/RT) versus (σ/G) data from compression creep experiments and (VT/Gφ)exp(Q/RT) versus (σ $_p$/G) from the impres-

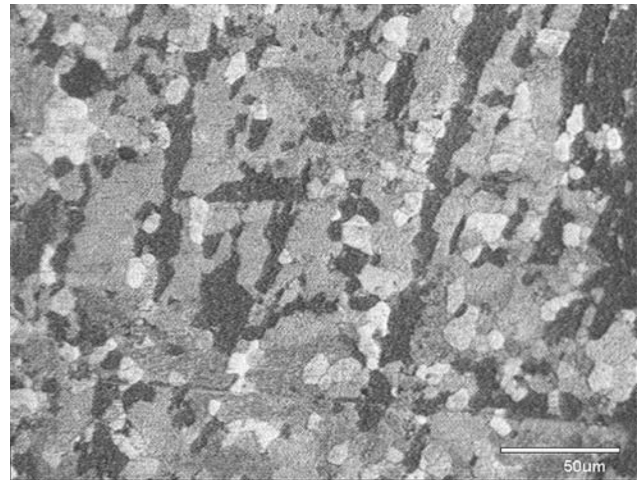

Fig. 1 Microstructure of polycrystalline Sn sample used for both impression and compression testing

[1] The punch stresses used in the impression creep tests were about three times larger than the corresponding stresses utilized in the compression creep tests, since σ_p~ 3σ [15–21].

[2] The curve fit produces a correlation coefficient R = 0.891 with n = 5.076. The error in A_{imp} is ±1.74 × 10^{11} K/(MPa-s).

[3] Since the Q calculation is based on only three experimental data points, it shows a large standard deviation (±10.18 kJ/mol), although the fit is reasonable (R = 0.97).

[4] The curve fit produces R = 0.892 with n = 5.05, the resultant error in A being ±1.58 × 10^{14} K/(MPa-s).

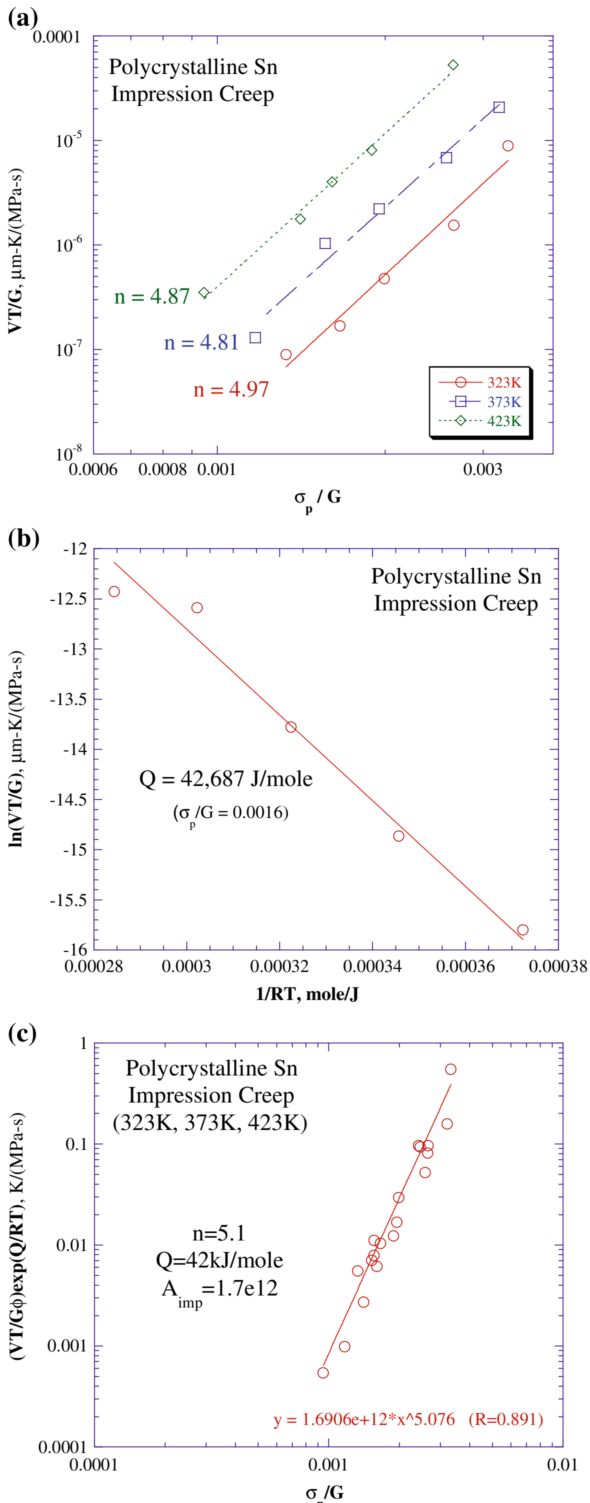

Fig. 2 Creep parameters obtained from impression creep test: (**a**) a plot of ln(VT/G) versus σ_p/G at different T values for computing n, (**b**) a plot of ln(VT/G) versus 1/RT at constant σ_p/G for computing Q, and (**c**) a plot of (VT/Gφ)*exp(Q/RT) versus σ_p/G for Q = 42 kJ/mol. The curve fit results show that n ~ 5.1 and A_{imp} ~ 1.7 × 10^{12} K/(MPa-s)

sion creep data, on the same plot frame. Both sets of data fit well with n = 5.1 and Q = 42 kJ/mol, with A = 1.6 × 10^{15} K/(MPa-s), for compression creep, and A_{imp} = 1.7 × 10^{12} K/(MPa-s) for impression creep, as shown by the dashed and solid lines, respectively. Thus the n and Q values obtained from the impression and compression creep tests are nominally identical.

The above n and Q values are also very close to previous impression creep studies on single crystal Sn along the [100] direction over 293–373 K [7], as well as tensile creep studies on [100] single crystals between 343 and 423 K [6]. For dislocation core diffusion controlled creep in single crystal Sn, Q values of 34–38 kJ/mol have been noted for creep along [110] and [001], and 40–50 kJ/mol for creep along [100] [3, 4, 6, 7]. Furthermore, activation energies of 39 and 44 kJ/mol have been noted in polycrystalline Sn and along [100] in single crystal Sn, respectively, in diffusion studies [25, 26]. It is therefore concluded that for polycrystalline Sn under the conditions of the present study, the creep mechanism is dislocation core diffusion controlled dislocation climb.

Since the n and Q values obtained via both impression and compression creep are identical, we may now obtain the conversion parameter κ^n/C for polycrystalline Sn, which is required to deduce the equivalent uniaxial creep behavior from impression creep data (i.e., to make the solid line representing the impression creep data in Fig. 4 translate and superimpose on the dashed line representing uniaxial creep data). By multiplying both sides of Eq. 6 by the constant (b/k), we have:

$$A_1\left(\frac{b}{k}\right) = \frac{A_2\kappa^n}{\phi C}\left(\frac{b}{k}\right), \text{ or } A = A_{imp}\left(\frac{\kappa^n}{C}\right) \tag{9}$$

Since and A_{imp} = 1.7 × 10^{12} K/(MPa-s), and 1.6 × 10^{15} K/(MPa-s), this yields $\kappa^n/C \approx 941$. Thus, following determination of n, Q and A_{imp} via impression creep testing, the equivalent uniaxial creep equation for polycrystalline Sn may be written as:

$$\dot{\varepsilon} = 941\, A_{imp}\left(\frac{G}{T}\right)\left(\frac{\sigma}{G}\right)^n e^{-Q/RT} \tag{10}$$

It should be noted that the value of the conversion constant (κ^n/C) is dependent on the material properties n and Q, but is relatively insensitive to the Dorn constant A_1 (Long X, Pan D, Dutta I, unpublished research, manuscript in review). Based on previous finite element simulations of the impression creep problem, (κ^n/C) may be empirically expressed as (Long

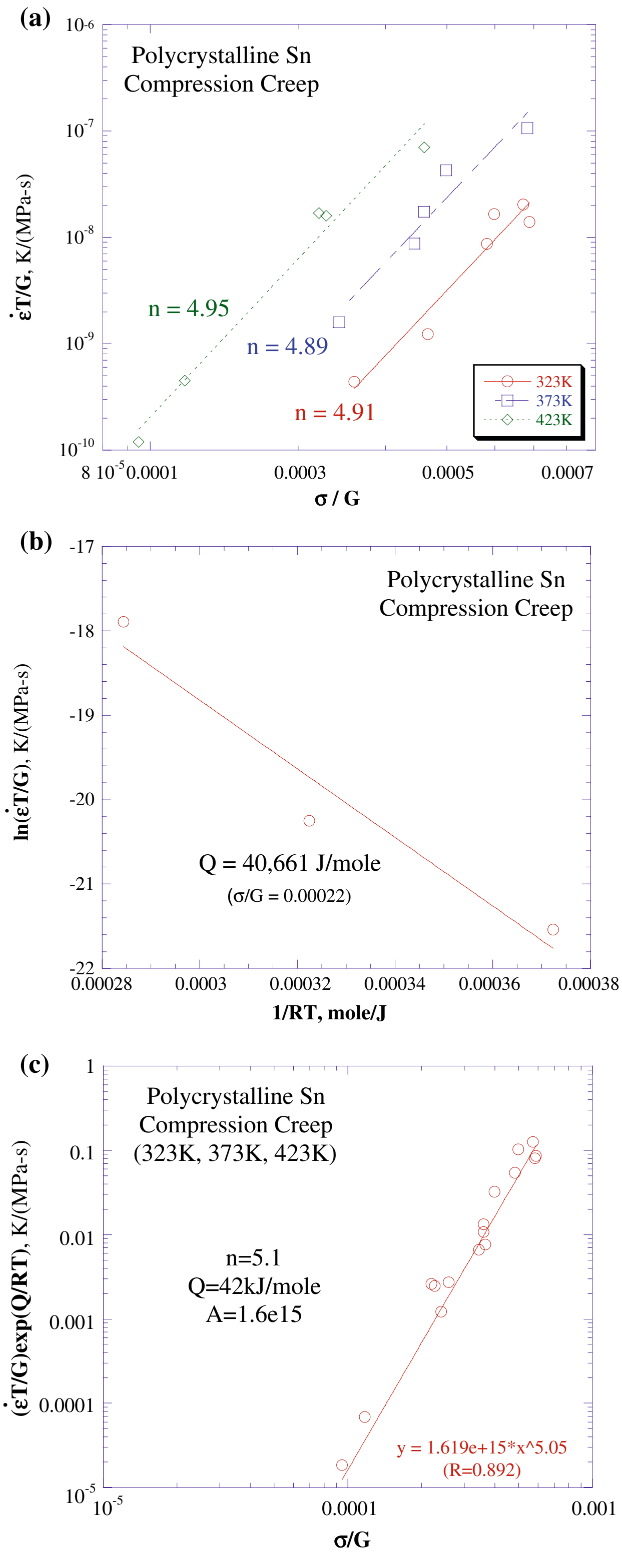

Fig. 3 Creep parameters obtained from compression creep test: **(a)** a plot of $\ln(\dot{\varepsilon}T/G)$ versus σ/G at different T values for getting n, **(b)** a plot of $\ln(\dot{\varepsilon}T/G)$ versus 1/RT at constant σ/G for obtaining Q, and, **(c)** a plot of $(\dot{\varepsilon}T/G) * \exp(Q/RT)$ versus σ/G for Q = 42 kJ/mol. The curve fit results show that n ~ 5.1 and A ~ 1.6×10^{15} K/(MPa-s)

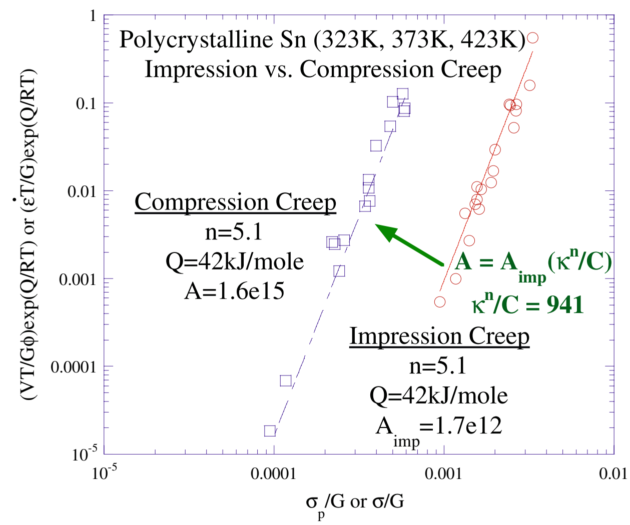

Fig. 4 Plots of $(\dot{\varepsilon}T/G)\exp(Q/RT)$ versus (σ/G) data from compression creep experiments and $(VT/G\varphi)\exp(Q/RT)$ versus (σ_p/G) from the impression creep data, on the same plot frame. Curve fits of both sets of data, using n = 5.1 and Q = 42 kJ/mol, with A = 1.6×10^{15} K/(MPa-s) for compression creep, and $A_{imp} = 1.7 \times 10^{12}$ K/(MPa-s) are also shown, and are observed to fit the respective data excellently. A conversion factor κ^n/C = 941 may be used to convert A_{imp} to A, enabling the impression creep data to superpose on the compression creep data

X, Pan D, Dutta I, unpublished research, manuscript in review):

$$\frac{\kappa^n}{C} \approx 2.75 \times 10^{-4} e^{1.35\,n}[7840 - 0.13Q + 5.7 \times 10^{-7}Q^2] \tag{11}$$

For the n and Q values of the present work, Eq. 8 gives $\kappa^n/C \approx 910$, which is close to the experimental κ^n/C value of 941 obtained here (within ~3%), thereby providing experimental validation of Eq. 11.

Conclusions

In conclusion, the creep parameters of polycrystalline Sn were determined via impression and compression creep are identical, with n ~ 5 and Q ~ 42 kJ/mol, indicating that over the tested stress–temperature range, the mechanism is core diffusion controlled dislocation creep. A single conversion factor, κ^n/C, which depends on material properties, may be used to convert the impression creep relation (impression velocity versus punch stress) to the equivalent uniaxial creep relation (strain rate versus stress). For polycrystalline Sn, the experimental value of κ^n/C, which equals 941, is close to the predicted value of 910 for the same material, based on previous modeling work.

Acknowledgements This work is supported by an NSF-GOALI program in partnership INTEL Corporation (Grant # DMR-0209464) and SRC contract # 2002-NJ-1004.

References

1. Dutta I, Park C, Choi S (2004) Mater Sci Eng A379:401
2. Mathew MD, Yang H, Movva S, Murty KL (2005) Metall Mater Trans 36A:99
3. Breen JE, Weertman J (1955) J Metals 1230
4. Adeva P, Caruanna G, Ruano OA, Torralba M (1995) Mater Sci Eng A194:17
5. Frenkel RE, Sherby OD, Dorn JE (1955) Acta Metall 3:470
6. Suh SH, Cohen JB, Weertman J (1983) Metall Trans 14A:117
7. Chu SNG, Li JCM (1979) Mater Sci Eng A39:1
8. Song HG, Morris JW, Hua F (2002) Mater Trans (Japan) 43:184
9. Pan D, Marks RA, Dutta I, Mahajan R, Jadhav SG (2004) Rev Sci Instrum 75:5244
10. Pan D, Dutta I, Jadhav SG, Raiser GF, Ma S (2005) J Electron Mater 34:1040
11. Marks RA, Pan D, Dutta I, Jadhav SG (2004) Proc. 9th intersociety conf. on thermal and thermomechanical phenomena in electronic systems, IEEE/ASME, pp 95–102
12. Dutta I, Pan D, Jadhav S, Mahajan R (2005) Proc. InterPACK 2005 (Intl. Electronic Packaging Technology Conference), ASME, Paper No. 73408, pp 189–195
13. Yu EC, Li JCM (1977) Philos Mag 34:811
14. Li JCM (2002) Mater Sci Eng A322:23
15. Yu HY, Li JCM (1977) J Mater Sci 12:2214
16. Sargent PM, Ashby MF (1992) Mater Sci Technol 8:594
17. Yu HY, Imam MA, Rath BB (1995) In: Chu SNG, Liaw PK, Arsenault RJ, Sadananda K, Chan KS, Gerberich WW, Chau CC, Kung TM (eds) Micromechanics of advanced materials. The Materials Metals & Materials Society
18. Yu HY, Imam MA, Rath BB (1985) J Mater Sci 20:636
19. Sastry DH, Murthy GS (1986) Trans Ind Inst Met 39:369
20. Gondi P, Sili A (1991) Z Metall 82:377
21. Chinh NQ, Tasnadi P, Juhasz A, Szommer P, Szep-Kiss E, Kovacs I (1994) Key Eng Mater 97–98:159
22. Yang FQ, Li JCM, Shih CW (1995) Mater Sci Eng A201:50
23. Hyde TH, Yehia KA, Becker AA (1993) Int J Mech Sci 35:451
24. Vianco PT, Rejent JA, Kilgo AC (2003) J Electron Mater 32:142
25. Bokshtein SZ (Samuil Zeilikovich) (1961) Investigation of the structure of metals by radioactive isotope methods. State Publishing House, Moscow
26. Fensham PJ (1950) Austr J Sci Res 3A:99